LASER & PHOTONICS REVIEWS

www.lpr-journal.org

Humidity-Induced Reversible Crystallization of Laser-Printing Perovskite Quantum Dots in Glass

*Han Xiao, Jidong Lin, Ronghua Chen, Tao Pang, Ping Huang, Yunlong Yu, Bin Zhuang, Qingying Ye, Ruidan Zhang, and Daqin Chen**

The complex and high-precision patterning of perovskite quantum dots (PeQDs) is of vital importance for exploring their new functionalities and device applications. In this work, a strategy based on the combination femtosecond (fs) laser-irradiation and humidity-control is reported to construct patterns of cyan $CsPb(Cl/Br)_3$ PeQDs in a transparent glass medium. Benefiting from their ionic crystal feature and low formation energy, $CsPb(Cl/Br)_3$ PeQDs can be locally crystallized and decomposed via fs laser irradiation without further heat-treatment. More notably, it is found that a water molecule is able to affect the growth of $CsPb(Cl/Br)_3$ PeQDs in glass. By modulation of relative humidity in air, the selectively decomposed perovskite structure is spontaneously regenerated, and the highly emissive $CsPb(Cl/Br)_3$ PeQDs can be in situ manufactured in the confined glass region. This allows for reversible luminescence from the same patterns of laser printing-erasing-recovering, and the process can be repeated for multiple cycles without destruction of optical performance and robustness. The results provide a flexible method to develop new encryption/decryption technology for information security and anti-counterfeiting.

1. Introduction

Perovskite quantum dots (PeQDs) have become one of the hottest materials for the applications in the optoelectronic devices, such as light-emitting diodes (LEDs),[1–6] photodetectors,[7,8] solar cells,[9,10] and lasers.[11–15] Due to their ionic crystal feature and low formation energy,[16,17] PeQDs suffer from decomposition under the influence of oxygen, moisture, temperature and light,[18–20] but show the advantage of being easy fabrication regardless of in solution or solid state. Such unique properties motivate us to explore a new and convenient approach to reversibly fabricate/decompose PeQDs but remain their structural stability, which is highly desirable for the applications in high-throughput optical information encryption/decryption and data storage.

Incorporating PeQDs into robust inorganic glass can enhance their photothermal stability and moisture resistance without fussy steps. So far, three kinds of methods have been reported to synthesize PeQDs glasses.[21] Generally, PeQDs can be nucleated/grown inside glass by in situ crystallization (heat-treatment).[22–24] The second way is realized via low-temperature co-sintering the pre-prepared PeQDs and low-melting glasses. Interestingly, pattern luminescent structures can be produced within the co-sintering perovskite glass via a facile cw laser irradiation.[25] The third one is to directly induce the nucleation/growth of PeQDs by pulse laser irradiation after the glass quenching. Recently, femtosecond (fs) laser direct writing has been shown to be an effective way to induce local crystallization of PeQDs within glass matrix. This high spatial resolution of processing is achieved by strong photon-matter interaction with transparent glass through nonlinear multiphoton absorption, resulting

H. Xiao, J. Lin, R. Chen, B. Zhuang, Q. Ye, R. Zhang, D. Chen
College of Physics and Energy
Fujian Normal University
Fuzhou, Fujian 350117, P. R. China
E-mail: dqchen@fjnu.edu.cn

T. Pang
Huzhou Key Laboratory of Materials for Energy Conversion and Storage
College of Science
Huzhou University
Huzhou, Zhejiang 313000, China

P. Huang
State Key Laboratory of Structural Chemistry
Fujian Institute of Research on the Structure of Matter
Chinese Academy of Sciences
Fuzhou 350002, China

Y. Yu
Organic Optoelectronics Engineering Research Center of Fujian's Universities
Fujian Jiangxia University
Fuzhou 350108, P. R. China

D. Chen
Fujian Provincial Collaborative Innovation Center for Advanced High-Field Superconducting Materials and Engineering
Fuzhou, Fujian 350117, P. R. China

D. Chen
Fujian Provincial Engineering Technology Research Center of Solar Energy Conversion and Energy Storage
Fuzhou, Fujian 350117, P. R. China

The ORCID identification number(s) for the author(s) of this article can be found under https://doi.org/10.1002/lpor.202300705

DOI: 10.1002/lpor.202300705

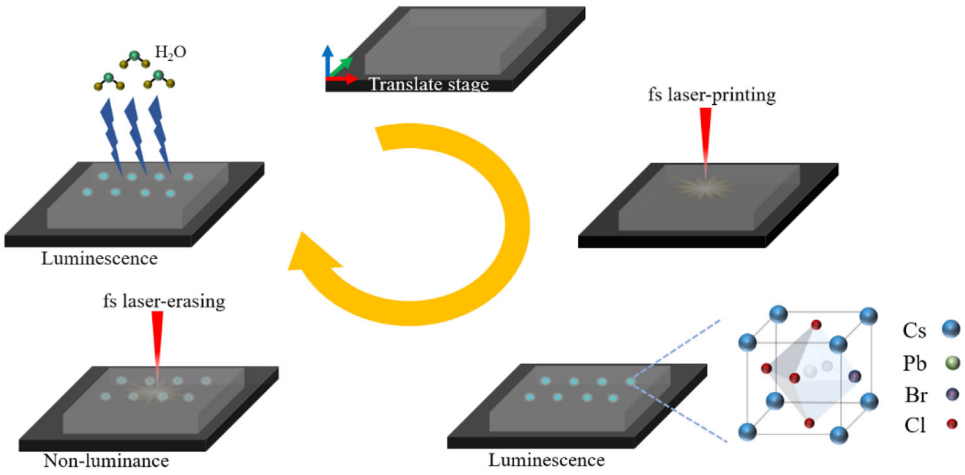

Scheme 1. Schematic illustration of fs laser-induced formation - erasing - recovery of CsPb $(Cl/Br)_3$ PeQDs in transparent glass medium.

in destruction of glass network structure and rapid redistribution of atoms around the laser focus, which facilitates ion migration to form PeQDs at a low crystallization temperature. For example, 3D direct lithography of composition-tunable PeQDs by fs laser-induced liquid nanophase separation and writing/erasing PeQDs patterns in glass by varying laser parameters have been reported previously. [26–28] However, an additional heat treatment is necessary to promote growth of the nuclei and induce their luminescence, which to some extent brings inconvenience to the operation and affects their practical application.

Herein, we report that cyan $CsPb(Cl/Br)_3$ PeQDs can be generated/erased in a well-designed glass via fs laser printing without the requirement of heat-treatment for the first time. Importantly, another affecting factor of humidity is found to enable to induce recovery of PeQDs decomposed by fs laser irradiation. By placing the laser-erasing glass in the air for a certain time, photoluminescence (PL) in the erased region can be recovered without further annealing, showing good optical performance and robustness, as shown in **Scheme 1**. In combination with a computer-controlled three-axis XYZ translation stage, complex and fine patterns within a glass substrate enables reversible in situ laser manufacturing, achieving reversible cryptographic reading and repeatable erasing/refreshing of multimodal information encryption. This technology will have potential applications in 3D displays, optical data storage, and information security.

2. Results and Discussion

A borosilicate glass containing Cs, Pb, Cl, and Br elements is designed for the laser-induced formation of $CsPb(Cl/Br)_3$ PeQDs. Heat-treatment is a routine way to induce PeQDs crystallization in glass. Herein, X-ray diffraction (XRD) patterns (Figure S1, Supporting Information) show that glass samples after thermal treatment from 450 to 600 °C exhibit only amorphous halo without apparent crystallization peak. The results suggest that the crystallization of $CsPb(Cl/Br)_3$ PeQDs in the present glass cannot be achieved directly by heat-treatment. In comparison, fs laser irradiation with a central wavelength of 1030 nm, a repetition frequency of 10 kHz, and a pulse duration of 300 fs can induce the formation of $CsPb(Cl/Br)_3$ PeQDs. When the fs laser pulse is tightly focused inside the glass, various nonlinear effects are induced, energy is transferred to the lattice through electron-phonon coupling, the temperature of the laser focusing region rises drastically, the heat accumulation changes the surrounding materials, and the glass network structure collapses locally, which are favorable for the migration of atoms to grow PeQDs.[26,27] Absorption spectra, X-ray photoelectron spectroscopy (XPS) and Raman spectra of precursor glass (PG) without/with fs laser irradiation were measured. The glass irradiated by fs laser has an obvious exciton absorption peak (Figure S2, Supporting Information). From the high-resolution XPS spectra (Figure S3, Supporting Information), it can be seen that the binding energy of Cs, Pb, Cl, and Br elements all shows a slight shift compared to the precursor glass. Several Raman signals at 72, 187, and 277 cm^{-1} are discerned (Figure S4, Supporting Information), which are assigned to vibration of $[PbBr_6]^{4-}$ octahedron, $[PbCl_6]^{4-}$ octahedron, and torsional vibration of Cs^+ coupling to $[PbBr_6]^{4-}$ and $[PbCl_6]^{4-}$ octahedrons, respectively.[29–33] All these results verify that $CsPb(Cl/Br)_3$ PeQDs can be generated in glass after fs laser irradiation.

As shown in **Figure 1**a, after fs laser irradiation, the formation of regularly shaped dot around the laser focal spot is observed in an optical microscope. With increase of laser pulse energy and extension of exposure time, its size continuously enlarges. Under the excitation of 365 nm ultraviolet (UV) lamp, the bright cyan PL can be well confined within laser irradiated area (Figure 1b). The emissive intensity mapping clearly reflects the generation of $CsPb(Cl/Br)_3$ PeQDs (Figure 1c). PL spectra of the laser irradiated region with a pulse energy of 200 μJ at different exposure times are exhibited in Figure 1d. PL peak position is limited within the range of 490–500 nm (Figure 1e), indicating that the size of the $CsPb(Cl/Br)_3$ PeQDs slightly varies. The formation of $CsPb(Cl/Br)_3$ PeQDs in glass is affected by the pulse energy and exposure time of the laser. Increasing the pulse energy and extending the exposure time contribute to emitting more intense PL (Figure 1f). Additionally, the line of $CsPb(Cl/Br)_3$ PeQDs is written by changing the displacement speed of the sample platform (Figure S5, Supporting Information). As the stage movement speed increases, the width of the line becomes narrower (Figure S5, Supporting Information) and the corresponding

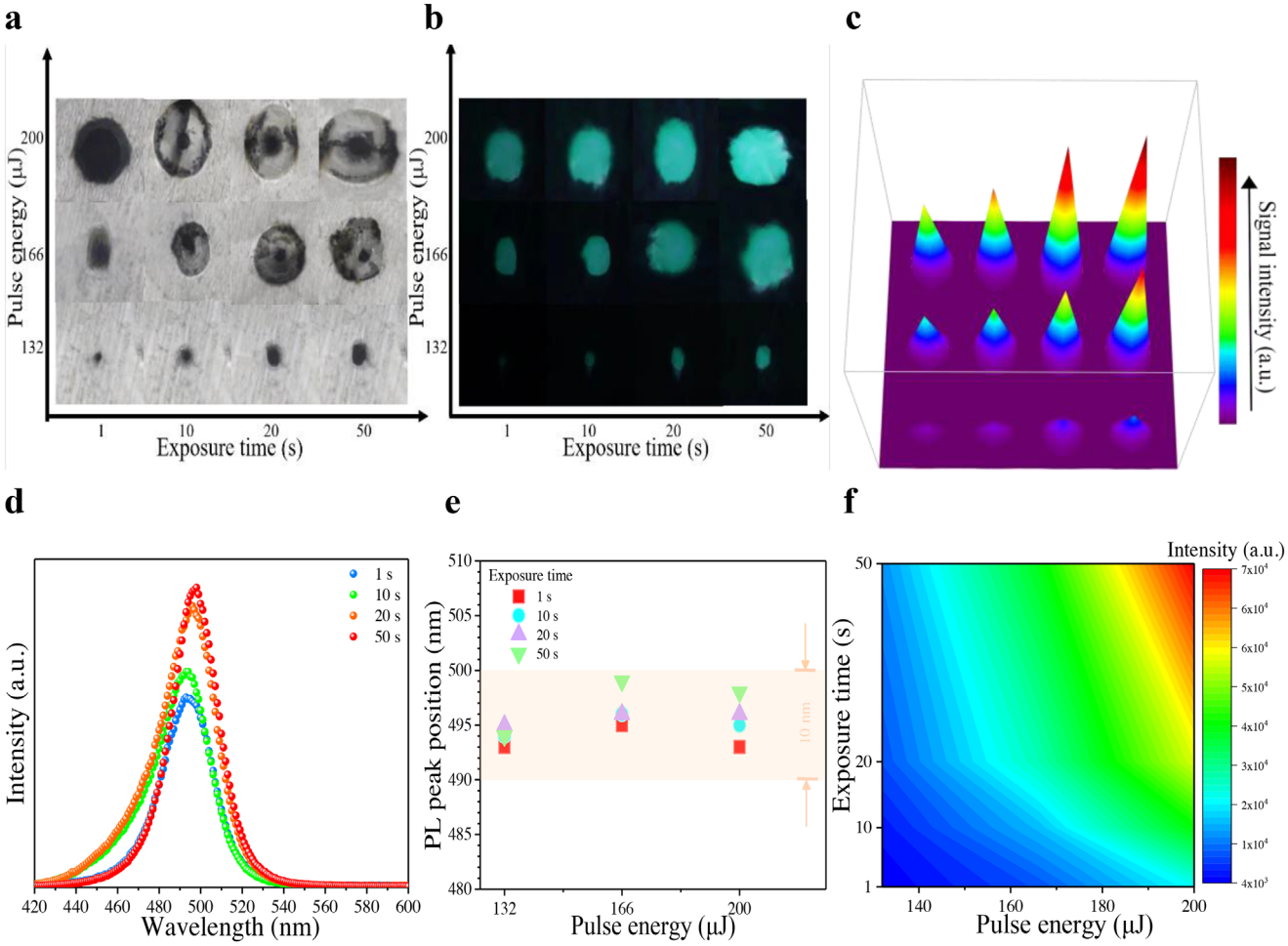

Figure 1. a,b) Optical images taken under an optical microscope and under 365 nm UV light of fs laser irradiated areas generated by using different pulse energies and exposure times. c) Emission signal intensity map corresponding to (b). d) Typical PL spectra of the laser irradiated region fabricated by a laser pulse energy of 200 μJ and different exposure times. e,f) PL peak position and PL intensity map in the laser irradiated region created by using different laser pulse energies and exposure times (λ_{ex} = 365 nm).

PL intensity becomes weakened (Figure S6, Supporting Information). Accordingly, the optimal laser parameters with a pulse energy of 200 μJ, repetition frequency of 10 kHz, average power of 500 mW and moving speed of 0.4 mm $^{-1}$s are adopted in the present work. Absorption, PL excitation (PLE), PL spectra, and decay curve of the laser-printing glass, as shown in Figure S7 (Supporting Information), exhibit typical exciton recombination feature of PeQDs with a decay lifetime in a nanosecond scale.

Laser-induced $CsPb(Cl/Br)_3$ PeQDs can be selectively erased by further fs laser irradiation (**Figure 2**a). The pulse energy used in our experiment to erase the preformed pattern can be lowered down to 30 μJ, and the exposure time can be shortened to 1 s. We can see from the figure that after being erased, the PL intensity of the glass is quenched, and under the irradiation of the 365 nm UV lamp, the laser irradiated area does not emit light. Interestingly, by leaving the glass in the air for 30 min (without any heat-treatment process), the PL intensity returns to almost the same as the original one (Figure 2a). In addition, cycle laser erasing and recovery process is carried out to demonstrate that fs laser irradiation and in situ placement in the air (relative humidity of 40–50% for 30 min) can achieve switchable PL of $CsPb(Cl/Br)_3$ PeQDs (Figure 2b). The PL intensity and the full width at half-maximum (fwhm) of $CsPb(Cl/Br)_3$ PeQDs generated during the cycling processes fluctuates within a small range, and the PL peak position remains in the range of 490–500 nm, indicating that the growth process of $CsPb(Cl/Br)_3$ PeQDs in glass is completely reversible.

To investigate structural changes of $CsPb(Cl/Br)_3$ PeQDs in glass during laser erasing/recovery, transmission electron microscope (TEM) images (Figure 2c–e), Raman spectra (Figure 2f) and absorption spectra (Figure 2g) were recorded. Apparently, a crystal phase with an interplanar distance of 0.27 nm assigned to (200) plane of PeQDs is observed from the high-resolution transmission electron microscopy (HRTEM) image taken in the laser writing region (Figure 2c), and the average size is evaluated to be 2.64 nm (Figure S8a, Supporting Information). When using fs laser for erasing, an obvious change is that the $CsPb(Cl/Br)_3$ PeQDs disappear in the image of the laser erased area (Figure 2d). PeQDs is easy to decompose when exposing to light, resulting in serious damage to the crystal structure of $CsPb(Cl/Br)_3$.

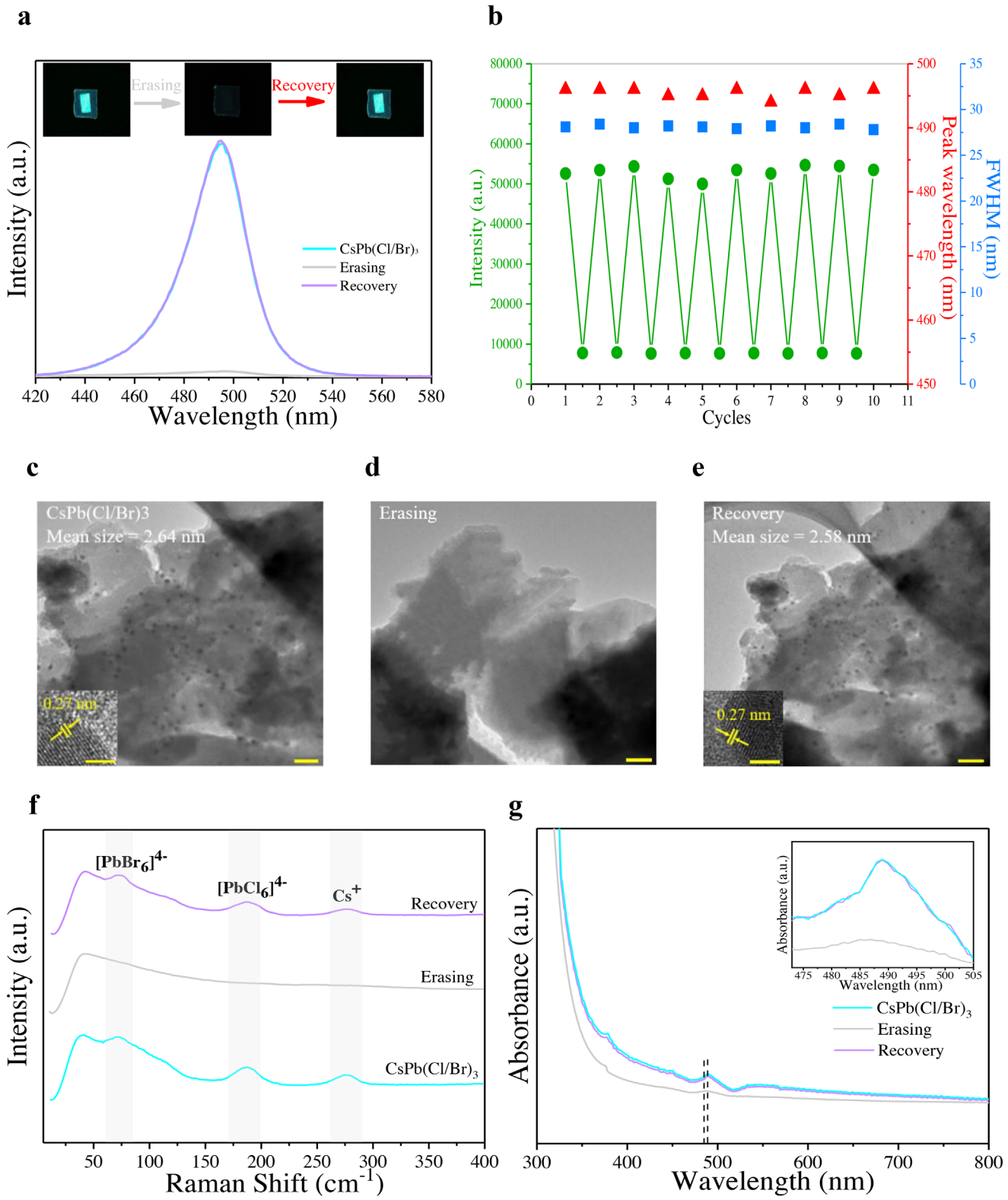

Figure 2. a) Switchable PL spectra and optical images for $CsPb(Cl/Br)_3$ PeQDs generated in glass recorded during one cycle of the erasing/recovery process under the excitation of 365 nm UV light. b) PL intensity, PL peak position and fwhm of $CsPb(Cl/Br)_3$ PeQDs recorded during nine continuous cycles of the erasing/recovery process. c–e) TEM and HRTEM images of $CsPb(Cl/Br)_3$ PeQDs taken for an erasing/recovery cycle. Scale bars in c–e): 10 nm, and scale bars in insets of c,e): 1 nm. f) Raman spectra and g) absorption spectra of $CsPb(Cl/Br)_3$ PeQDs in glass recorded during one cycle of the erasing/recovery process. The inset in (g) is the enlarged absorption spectra in the region of 470 to 505 nm.

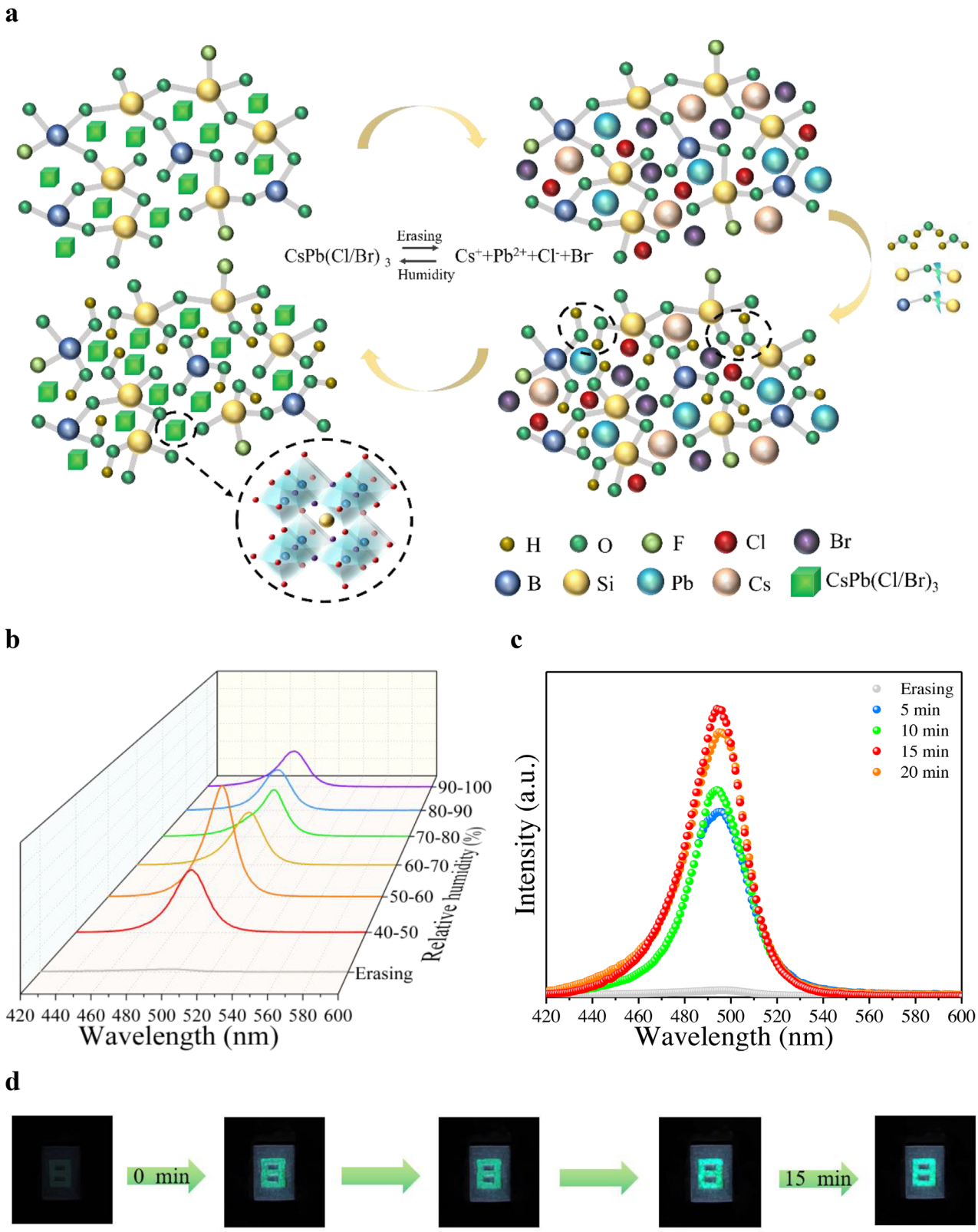

Figure 3. a) Schematic diagram of variation of glass network structure to illustrate the erasing/recovery mechanism of $CsPb(Cl/Br)_3$ PeQDs in glass after fs laser irradiation and water invasion. b) PL spectra of fs laser-erasing glass placed in different relative humidity environments for 15 min. c) PL spectra of fs laser-erasing glass placed in the environments with relative humidity of 50–60% at different times. d) Demonstration of the gradual recovery of the erased $CsPb(Cl/Br)_3$ PeQDs pattern placed in an environment with a relative humidity of 50–60% for 15 min.

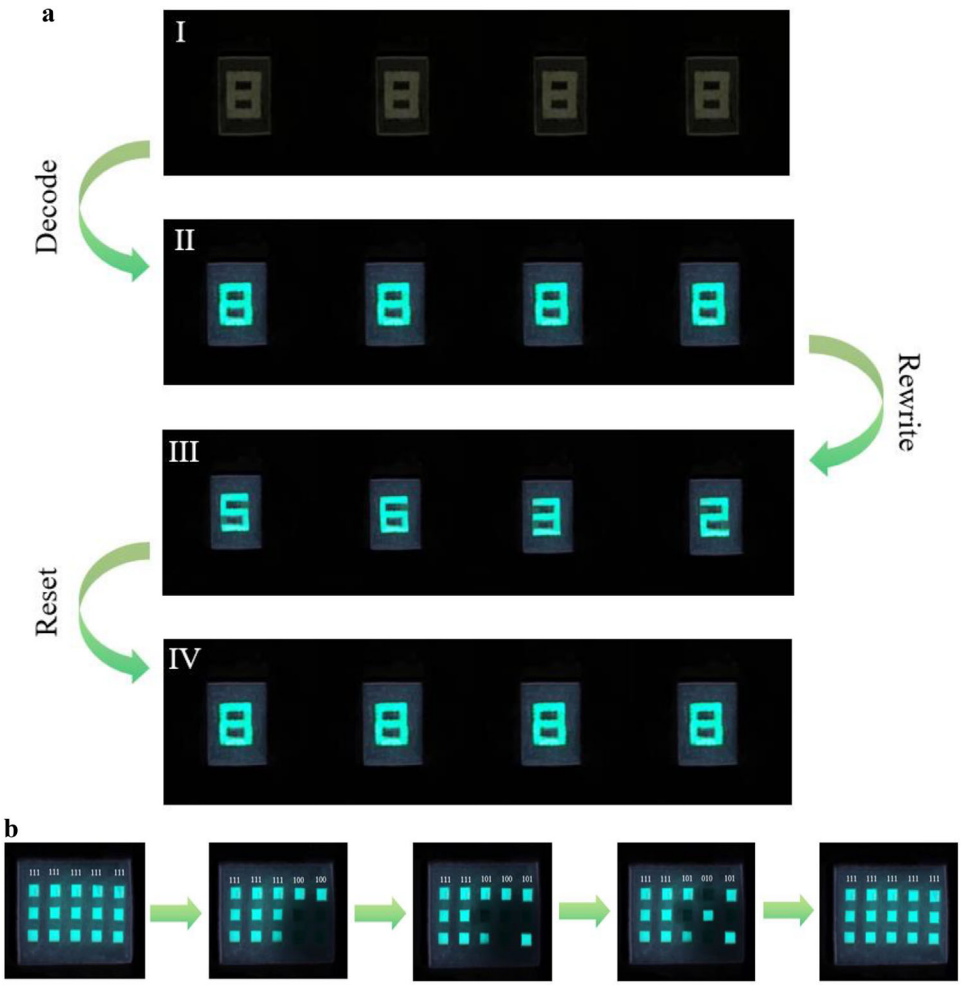

Figure 4. a) Demonstration of erasable patterning of $CsPb(Cl/Br)_3$ PeQDs in glass for information encryption and decryption. b) Demonstration of erasable patterning of $CsPb(Cl/Br)_3$ PeQDs in glass for binary encoding and decoding.

Accordingly, after low-power fs laser irradiation, it can be observed that the Raman peak intensities at 72, 187, 277 cm^{-1} become significantly weakened (Figure 2f). The exciton absorption peak of $CsPb(Cl/Br)_3$ PeQDs also decreases accompanied with blueshifting after erasing (Figure 2g), which can provide further favorable evidence for the laser-degradation of $CsPb(Cl/Br)_3$ PeQDs. Subsequently, by placing the glass in the air environment for some durations (30 min), $CsPb(Cl/Br)_3$ PeQDs with size of 2.58 nm (Figure 2e; Figure S8b, Supporting Information), and the corresponding Raman peaks and the exciton absorption signal reappear (Figure 2f,g).

To find out exact mechanism of PeQDs self-recovery in air, comparison experiments are carried out (Figure S9, Supporting Information). When the laser-erasing glass is placed in a vacuum environment, the glass does not emit light; when a little water is sprayed on the glass, cyan emission appears; However, if a large amount of water is used, the luminescence is quenched again. Accordingly, it is believed that water molecules in the air indeed affect the regeneration of laser-erasing $CsPb(Cl/Br)_3$ PeQDs in glass. The possible erasing/recovery mechanism of PeQDs in glass is proposed in **Figure 3**a. After fs laser erasing, $CsPb(Cl/Br)_3$ PeQDs will be decomposed into Cs^+, Pb^{2+}, Br^- ,and Cl^- ions confined within the interstitial sites of glass network interstitial site. Notably, the employed borosilicate glass is one of the most humidity resistant glasses. As evidenced in Figure S1 (Supporting Information), $CsPb(Cl/Br)_3$ PeQDs could not be crystallized in the present glass by direct heat-treatment, indicating that the network depolymerization induced by the addition of network modifiers in the glass is not enough for the nucleation/growth of PeQDs. We should mention clearly that the employed laser focal point is located on the glass surface in the present work. Therefore, the interaction between fs laser and glass causes micro-cracks, and when water molecules in the air come into contacting with the glass surface due to thermal movement, the glass structure will be destroyed. Under the continuous invading of H^+ and OH^-, the bridge oxygen in the Si—O—Si and B—O—Si bonds will be broken, leading to further depolymerization of the borosilicate glass structure. [34] This will provide sufficient space for ion migration in glass network and significantly decrease recovery activation energy of PeQDs. As a result, benefiting from ionic crystal feature of halide perovskite and confined region in glass irradiated by fs laser, the network modifiers Cs^+,

Pb^{2+}, Br^-, Cl^- spontaneously aggregate and crystallize to regenerate $CsPb(Cl/Br)_3$ PeQDs. To validate the proposed mechanism, the laser-erasing glass is placed in an environment with different relative humidity. Indeed, PL of the glass is sensitive to relative humidity, and PL intensity reaches maximum for the glass treated under the 50–60% relative humidity (Figure 3b). With elevation of relative humidity, the PL peak position shows a redshift, which indicates the growth of $CsPb(Cl/Br)_3$ crystal. However, when the relative humidity exceeds 80%, the PL peak appears a blueshift and PL begins to quench, indicating that excessive water will destroy/decompose PeQDs (Figure S9, Supporting Information). In addition, on this basis, the best time to place in the optimal relative humidity of 50–60% is evidenced to be 15 min (Figure 3c). To verify that highly tunable humidity can promote the growth of PeQDs, the preformed pattern after erasing is placed in an environment with relative humidity of 50–60% for 15 min (Figure 3g). It can be seen that the digital "8" pattern gradually recovers with the elongation of humidity treatment time, and its brightness can be completely restored after 15 min.

As a demo, this humidity-induced reversible crystallization of laser-printing PeQDs in glass is used in the application of information encryption/decryption. First, four seven-segment numerical codes are constructed (**Figure 4**a). Laser directly lithographs the digital "8" patterns in the glass (Figure 4a-I), which are not visible by the naked eyes in daylight and can only be decoded when illuminated by a UV lamp (Figure 4a-II). Then, a low-power fs laser can easily erase certain specific segments to rewrite the codes (Figure 4a-III), which are spontaneously reset in air environment for few minutes (Figure 4a-IV). Furthermore, the application of the technique in binary code is also demonstrated, where bright state and dark ones represent "1" and "0", respectively, as shown in Figure 4b. Laser erasing can produce various kinds of binary codes, which can be recovered back to the original ones after putting in air for a certain time. Notably, the high robustness of the glass substrate ensures that the laser printing-erasing-recovery process can be repeated for several times (Figure S10, Supporting Information). This optical encryption technology improves the reliability and security of information, and it is believed that it will be widely used in the next generation of information security technology.

3. Conclusion

In summary, we have demonstrated the generating, erasing, and recovering of cyan $CsPb(Cl/Br)_3$ PeQDs in a transparent glass medium through fs laser printing and humidity controlling. Compared to previous laser writing in glass that requires subsequent heat-treatment, the one-step generation of $CsPb(Cl/Br)_3$ PeQDs in the specially designed glass is reported for the first time. More interestingly, the laser-erased $CsPb(Cl/Br)_3$ PeQDs can be autonomously regenerated in the confined glass region after exposing in air environment for a certain time owing to the depolymerization of the borosilicate glass structure by the invasion of water molecules and the promotion of in situ perovskite crystallization confined in the glass surface regions. Compared to the cases previously reported, the reversible crystallization of $CsPb(Cl/Br)_3$ PeQDs is achieved by in situ laser-erasing and humidity-recovering, avoiding cumbersome operating steps, which is demonstrated to be applicable for information encryption/decryption.

Supporting Information

Supporting Information is available from the Wiley Online Library or from the author.

Acknowledgements

This research was supported by the National Natural Science Foundation of China (52272141, 51972060, 12074068, 52102159, and 22103013), the Natural Science Foundation of Fujian Province (020J02017, 2022J05091, 22021J06021, 2021J01190, and 2020J01931), and the Organic Optoelectronics Engineering Research Center of Fujian's Universities, Fujian Jiangxia University (Grant No. JXKFA202201).

Conflict of Interest

The authors declare no conflict of interest.

Data Availability Statement

Research data are not shared.

Keywords

$CsPbX_3$, femtosecond laser, glass, luminescence, optical materials

Received: July 27, 2023
Revised: October 8, 2023
Published online:

[1] X. Li, Y. B. Zhao, F. Fan, L. Levina, M. Liu, R. Quintero-Bermudez, X. Gong, L. N. Quan, J. Fan, Z. Yang, S. Hoogland, O. Voznyy, Z. H. Lu, E. H. Sargent, *Nat. Photonics* **2018**, *12*, 159.
[2] Z. Li, Z. Chen, Y. Yang, Q. Xue, H. L. Yip, Y. Cao, *Nat. Commun.* **2019**, *10*, 1027.
[3] K. Lin, J. Xing, L. N. Quan, F. P. G. De Arquer, X. Gong, J. Lu, L. Xie, W. Zhao, D. Zhang, C. Yan, W. Li, X. Liu, Y. Lu, J. Kirman, E. H. Sargent, Q. Xiong, Z. Wei, *Nature* **2018**, *562*, 245.
[4] J. Luo, X. Wang, S. Li, J. Liu, Y. Guo, G. Niu, L. Yao, Y. Fu, L. Gao, Q. Dong, C. Zhao, M. Leng, F. Ma, W. Liang, L. Wang, S. Jin, J. Han, L. Zhang, J. Etheridge, J. Wang, Y. Yan, E. H. Sargent, J. Tang, *Nature* **2018**, *563*, 541.
[5] Y. Wei, Z. Cheng, J. Lin, *Chem. Soc. Rev.* **2019**, *48*, 310.
[6] L. Zhao, Y. W. Yeh, N. L. Tran, F. Wu, Z. Xiao, R. A. Kerner, Y. L. Lin, G. D. Scholes, N. Yao, B. P. Rand, *ACS Nano* **2017**, *11*, 3957.
[7] Q. Chen, J. Wu, X. Ou, B. Huang, J. Almutlaq, A. A. Zhumekenov, X. Guan, S. Han, L. Liang, Z. Yi, J. Li, X. Xie, Y. Wang, Y. Li, D. Fan, D. B. L. Teh, A. H. All, O. F. Mohammed, O. M. Bakr, T. Wu, M. Bettinelli, H. Yang, W. Huang, X. Liu, *Nature* **2018**, *561*, 88.
[8] H. Gao, J. Feng, Y. Pi, Z. Zhou, B. Zhang, Y. Wu, X. Wang, X. Jiang, L. Jiang, *Adv. Funct. Mater.* **2018**, *28*, 46.
[9] N. J. Jeon, H. Na, E. H. Jung, T. Y. Yang, Y. G. Lee, G. Kim, H. W. Shin, S. Il Seok, J. Lee, J. Seo, *Nat. Energy* **2018**, *3*, 682.
[10] E. H. Jung, N. J. Jeon, E. Y. Park, C. S. Moon, T. J. Shin, T. Y. Yang, J. H. Noh, J. Seo, *Nature* **2019**, *567*, 511.

[11] F. Fan, O. Voznyy, R. P. Sabatini, K. T. Bicanic, M. M. Adachi, J. R. Mcbride, K. R. Reid, Y. S. Park, X. Li, A. Jain, R. Quintero-Bermudez, M. Saravanapavanantham, M. Liu, M. Korkusinski, P. Hawrylak, V. I. Klimov, S. J. Rosenthal, S. Hoogland, E. H. Sargent, *Nature* **2017**, *544*, 75.
[12] J. Feng, X. Yan, Y. Zhang, X. Wang, Y. Wu, B. Su, H. Fu, L. Jiang, *Adv. Mater.* **2016**, *28*, 3732.
[13] Y. Jia, R. A. Kerner, A. J. Grede, B. P. Rand, N. C. Giebink, *Nat. Photonics* **2017**, *11*, 784.
[14] X. Li, Y. Wang, H. Sun, H. Zeng, *Adv. Mater.* **2017**, *29*, 36.
[15] B. Tang, H. Dong, L. Sun, W. Zheng, Q. Wang, F. Sun, X. Jiang, A. Pan, L. Zhang, *ACS Nano* **2017**, *11*, 10681.
[16] S. Zou, Y. Liu, J. Li, C. Liu, R. Feng, F. Jiang, Y. Li, J. Song, H. Zeng, M. Hong, X. Chen, *J. Am. Chem. Soc.* **2017**, *139*, 11443.
[17] X. K. Liu, W. Xu, S. Bai, Y. Jin, J. Wang, R. H. Friend, F. Gao, *Nat. Mater.* **2021**, *20*, 10.
[18] M. P. Arciniegas, A. Castelli, S. Piazza, S. Dogan, L. Ceseracciu, R. Krahne, M. Duocastella, L. Manna, *Adv. Funct. Mater.* **2017**, *27*, 34.
[19] S. Huang, Z. Li, B. Wang, N. Zhu, C. Zhang, L. Kong, Q. Zhang, A. Shan, L. Li, *ACS Appl. Mater. Interfaces* **2017**, *9*, 7249.
[20] G. Yuan, C. Ritchie, M. Ritter, S. Murphy, D. E. Gómez, P. Mulvaney, *J. Phys. Chem. C* **2018**, *122*, 13407.
[21] I. Konidakis, A. Karagiannaki, E. Stratakis, *Nanoscale* **2022**, *14*, 2966.
[22] S. Liao, Z. Yang, J. Lin, S. Wang, J. Zhu, S. Chen, F. Huang, Y. Zheng, D. Chen, *Adv. Funct. Mater.* **2023**, *33*, 2210558.
[23] S. Chen, J. Lin, S. Zheng, Y. Zheng, D. Chen, *Adv. Funct. Mater.* **2023**, *33*, 2213442.
[24] S. Chen, J. Lin, J. Huang, T. Pang, Q. Ye, Y. Zheng, X. Li, Y. Yu, B. Zhuang, D. Chen, *Adv. Funct. Mater.* **2023**, 2309293 https://doi.org/10.1002/adfm.202309293.
[25] I. Konidakis, K. Brintakis, A. Kostopoulou, I. Demeridou, P. Kavatzikidou, E. Stratakis, *Nanoscale* **2020**, *12*, 13697.
[26] K. Sun, D. Tan, X. Fang, X. Xia, D. Lin, J. Song, Y. Lin, Z. Liu, M. Gu, Y. Yue, J. Qiu, *Science* **2022**, *375*, 307.
[27] X. Huang, Q. Guo, S. Kang, T. Ouyang, Q. Chen, X. Liu, Z. Xia, Z. Yang, Q. Zhang, J. Qiu, G. Dong, *ACS Nano* **2020**, *14*, 3150.
[28] X. Huang, Q. Guo, D. Yang, X. Xiao, X. Liu, Z. Xia, F. Fan, J. Qiu, G. Dong, *Nat. Photonics* **2020**, *14*, 82.
[29] A. Bhardwaj, A. K. Kushwaha, *Appl. Phys. A-Mater. Sci. Process.* **2022**, *128*, 10.
[30] D. M. Calistru, L. Mihut, S. Lefrant, I. Baltog, *J. Appl. Phys.* **1997**, *82*, 5391.
[31] J. H. Cha, J. H. Han, W. Yin, C. Park, Y. Park, T. K. Ahn, J. H. Cho, D. Y. Jung, *J. Phys. Chem. Lett.* **2017**, *8*, 565.
[32] V. Dracopoulos, D. T. Kastrissios, G. N. Papatheodorou, *Polyhedron* **2005**, *24*, 619.
[33] M. Velázquez, A. Ferrier, S. Péchev, P. Gravereau, J. P. Chaminade, X. Portier, R. Moncorgé, *J. Cryst. Growth* **2008**, *310*, 5458.
[34] Y. Liu, X. Luo, S. Yang, D. Wang, H. Wu, Q. Wang, T. Han, C. Wang, D. Zhou, J. Qiu, *J. Am. Ceram. Soc.* **2022**, *105*, 4699.